ELSEVIER

Journal of Photochemistry and Photobiology A: Chemistry 155 (2003) 133–143

Journal of Photochemistry and Photobiology A:Chemistry

www.elsevier.com/locate/jphotochem

Photochemical and photocatalytic degradation of an azo dye in aqueous solution by UV irradiation

Cláudia Gomes da Silva, Joaquim Luís Faria*

Laboratório de Catálise e Materiais, Departamento de Engenharia Química, Faculdade de Engenharia da Universidade do Porto, Rua Dr. Roberto Frias 4200-465 Porto, Portugal

Received 10 October 2002; received in revised form 10 October 2002; accepted 18 October 2002

Abstract

The photochemical and photocatalytic degradation of aqueous solutions of Solophenyl Green (SG) BLE 155%, an azo dye preparation very persistent in heavy colored textile waters, has been investigated by means of ultraviolet (UV) irradiation. The pure photochemical process demonstrated to be very efficient for low initial concentrations of the dyestuff. For higher concentrations the photocatalyitic degradation was carried on using commercial titanium dioxide, and mixtures of this semiconductor with different activated carbons (AC) suspended in the solution. The kinetics of photocatalytic dyestuff degradation were found to follow a first-order rate law. It was observed that the presence of the activated carbon enhanced the photoefficiency of the titanium dioxide catalyst. Differently activated carbon materials induced different increases in the apparent first-order rate constant of the process. The effect was quantified in terms of a synergy factor (R) already described in the literature. The kinetic behavior could be described in terms of a modified Langmuir–Hinshelwood model. The values of the adsorption equilibrium constants for the organic molecules, K_C, and for the reaction rate constants, k_C, were 0.0923 l mg^{-1} and 1.58 mg l^{-1} min^{-1} for the TiO_2/UV process and 0.0928 l mg^{-1} and 2.64 mg l^{-1} min^{-1} for the TiO_2 + AC/UV system with highest synergy factor, respectively. The mechanism of degradation was discussed in terms of the titanium dioxide photosensitization by the activated carbon.

Keywords: UV photodegradation; Photochemistry; Photocatalysis; Titanium dioxide; Activated carbon; Azo dyes

1. Introduction

Removal of color in waste water from textile industries is a current issue of discussion and regulation all over the developed societies. Colored waters have a strong impact in the population and generate strong popular complaints. Allied to public relevance of the topic, the growing awareness that water will became a valuable asset in the future, prompted the scientific and technological communities for serious research on the domain of waste waters treatment and recycling. Because the costs involved are normally stringent for most of the medium to small size textile factories, so efficient and economic ways of treatment are sought. The attractiveness of the advanced oxidation processes (AOPs) [1–3] in providing a definite solution for the conversion of many organic (or inorganic oxidazible) compounds, lies in the fact that if they are used as tertiary treatment (specially in the textile industry) the resulting water can be recycled or re-used in a competitive way.

The development of AOPs based on ultraviolet (UV) photolysis, capable of mineralizing a wide range of recalcitrant or hazardous organic compounds, had a strong impact on the progress of the technology associated with photochemistry and photochemical processes.

A powerful and clean oxidizing agent is the UV radiation itself. It has a tremendous oxidation potential (a 253.7 nm photon provides 4.89 eV) which is normally enough to interact with the electronic structure of the matter. The degradation of the organic pollutant is normally initiated from an electronic excited state (Eq. (1)) which can undergo homolytic bond scission to form radicals that will react towards final products in a chain reaction with the participation (or not) of molecular oxygen (Eq. (2)), or initiate a process of electron transfer to a ground state oxygen molecule.

$$R \xrightarrow{h\nu} R^* \quad (1)$$

$$R^* \rightarrow R_1^{\bullet} + R_2^{\bullet} \rightarrow \text{products} \quad (2)$$

$$R^* + O_2 \rightarrow R^{\bullet +} + O_2^{\bullet -} \quad (3)$$

The resulting radical cation can undergo hydrolysis or mesolytic bond scission to low weight products. The

* Corresponding author. Tel.: +351-225-081-645; fax: +351-225-081-449.
E-mail address: jlfaria@fe.up.pt (J.L. Faria).

1010-6030/02/$ – see front matter
PII: S1010-6030(02)00374-X

superoxide radical ion ($O_2^{\bullet -}$) is known to be capable of degrading aromatic molecules. Although the emission of a low pressure Hg arc at 253.7 nm alone is not very effective for the removal of simple organics from water, more complex substituted aromatics with a more favorable absorption spectra can undergo efficient degradation.

The degradation capability of 253.7 nm irradiation can be enhanced in semiconductor mediated photocatalytic oxidation processes. After the first report on a titanium dioxide (TiO_2) application for the photocatalytic purification of waters containing cyanide [4,5], this material has been extensively used on environmental applications. What makes TiO_2 (specially in its anatase form) so attractive for this environmental applications are its attributes of photo-stability, non-toxicity, low cost and water insolubility under most conditions. The heterogeneous photocatalytic process is well described in the literature and has been subject of many reviews (examples are [6,7]) and reports concerning the technical aspects involved [8,9]. The process is initiated upon UV irradiation of the semiconductor with the formation of high energy state electron/hole pairs (e^-/h^+), which migrate to the surface, ready to initiate redox chemistries. Oxygen is present all over the TiO_2 and acts as electron acceptor to form the superoxide radical ion ($O_2^{\bullet -}$) while adsorbed OH^- groups and H_2O molecules are available as electron donors to yield the hydroxyl radical ($HO^{\bullet}$). Both species are strongly oxidizing and capable of degrading aromatic compounds.

$$(O_2)_{ads} + TiO_2(e^-) \rightarrow TiO_2 + O_2^{\bullet -} \quad (4)$$

$$(H_2O \rightleftarrows H^+ + OH^-)_{ads} + TiO_2(h^+) \rightarrow TiO_2 + H^+ + HO^{\bullet} \quad (5)$$

Some of the adsorbed aromatic compounds will also undergo direct oxidation by electron transfer to the surface holes.

$$R_{ads} + TiO_2(h^+) \rightarrow TiO_2 + R_1^{\bullet +} \quad (6)$$

The radical cation produced this way is prone to the same processes as described in the case of direct UV irradiation.

The high rate of electron/hole pair recombination reduces the quantum yield of the TiO_2 process and represents its major drawback. A way to possibly increase the photocatalytic efficiency of TiO_2 consists on adding a co-adsorbent such as activated carbon (AC). This effect has been explained by the formation of a common contact interface between the different solid phases, in which AC acts as an efficient adsorption trap to the organic pollutant, which is then more efficiently transferred to the TiO_2 surface where it is immediately photocatalytically degraded [10]. In the present paper, we examined the oxidative degradation of the azo dye Solophenyl Green (SG) BLE 155% by the described techniques.

Textile azo dyes [11] are pollutants of high environmental impact, because of their widespread use, their potential to form toxic aromatic amines and their low removal rate during primary and secondary treatment. They represent about 50% of the worldwide production and correspond to an important source of contamination considering that approximately 15% of the synthetic textile dyes are lost in waste streams during manufacturing or processing operations [12]. This work follows a series of case studies recently reported in literature [13–16] in which kinetic and mechanistic aspects of dye degradation are investigated with the aim of elucidating the potential applications of advantageous photocatalytic processes.

A series of works on the effects of adsorbents—mainly carbon—used as supports for TiO_2 in photocatalytic degradation reactions [17–19], attracted our initial attention to the fact that the conversion of organic pollutants could be drastically enhanced by this novel approach. More recent reports on the photocatalytic degradation of phenol [20,21] and other model pollutants [10], in aqueous suspended mixtures of TiO_2 and activated carbon, make reference to remarkable effects in the kinetics of disappearance of the pollutants, each pollutant being more rapidly photodegraded in the mixed system which contained activated carbon. This so designated synergy effect was explained by an important adsorption of the pollutants on the activated carbon followed by a mass transfer to the photoactive TiO_2. Different AC induce different effects suggesting that the properties of the co-adsorbent may play a significant role upon the photoefficiency of the associated TiO_2. This observation prompted us to study the effect of different types of activated carbons in the photocatalytic degradation of Solophenyl Green dyestuff.

2. Experimental

2.1. Materials

The Solophenyl Green BLE 155% dyestuff is an odorless green powder obtained from Ciba-Geigy (a gift from Ciba Portuguesa Lda) and was used as received. The thermal stability is guaranteed until 473 K and has a solubility in water of 10 g l^{-1} at 303 K. The UV-Vis spectrum of the aqueous solution of dyestuff at room temperature shows two absorption maxima at 382 and 610 nm. The molar absorption coefficients are, respectively, $\varepsilon_{382} = 28{,}950$ and $\varepsilon_{610} = 27{,}560\ M^{-1}\ cm^{-1}$, based on the given molecular weight of 1338 g mol^{-1} for a preparation containing the Solophenyl Green dye molecule (Fig. 1).

Titanium dioxide (Degussa P-25) was supplied by Degussa Portuguesa. The material is mainly anatase, with a BET surface area of 55 $m^2\ g^{-1}$ and a mean particle size of 30 nm (manufacturer data).

Three different commercial activated carbons from NORIT Nederland B.V. were used. Some were subjected to different chemical oxidation treatments as described in the following. All the carbon materials were ground to powder in a mortar prior to use. They were labeled as indicated next: AC1, a granular activated carbon (NORIT C GRAN) with a high adsorptive capacity, produced by

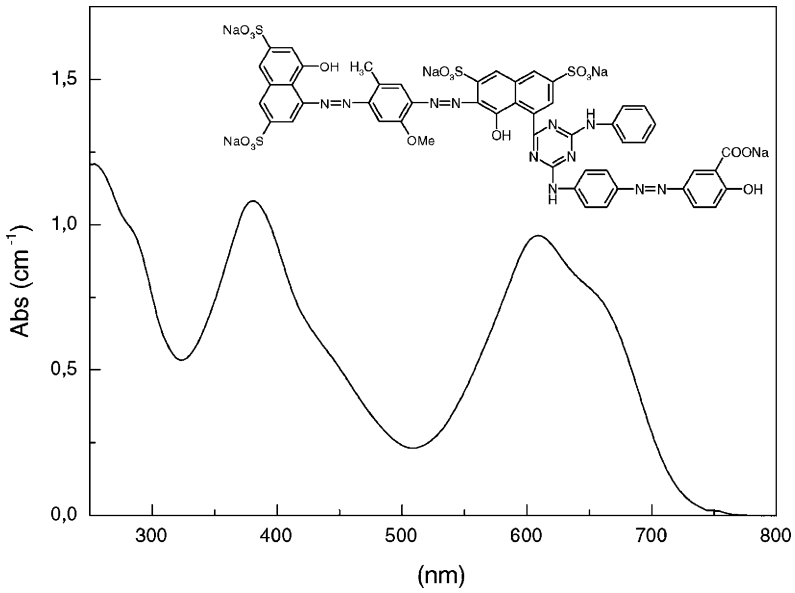

Fig. 1. Electronic absorption spectrum of the aqueous solution of Solophenyl Green BLE 155% dyestuff. Inset: Chemical structure of Solophenyl Green dye molecule.

chemical activation using the phosphoric acid process, having an open (macro/mesopore) porosity with a BET surface area of 1400 $m^2\,g^{-1}$ (supplier data); AC2, a granular activated carbon (NORIT GAC 1240 PLUS) acid washed with good adsorption properties and a very high purity, produced by steam activation, containing a BET surface area of 1000 $m^2\,g^{-1}$ and a total pore volume of 0.9 $ml\,g^{-1}$ (supplier data); AC3, an extruded activated carbon (NORIT ROX 0.8) acid washed, produced by steam activation and normally used in our laboratory for the preparation of carbon supported metal catalysts, having a BET surface area of 1100 $m^2\,g^{-1}$ (supplier data); AC4, AC3 oxidized in the liquid phase with 10 M solution of H_2O_2 at room temperature, determined BET surface area 908 $m^2\,g^{-1}$; AC5, AC3 oxidized in the liquid phase with 5 M nitric acid at the boiling temperature for 3 h, determined BET surface area 893 $m^2\,g^{-1}$; AC6, AC5 re-oxidized in a second stage with fresh 5 M nitric acid at the boiling temperature for another 3 h, determined BET surface area 833 $m^2\,g^{-1}$; AC7, AC5 treated under nitrogen at 973 K for 3 h, determined BET surface area 947 $m^2\,g^{-1}$; AC8, AC5 treated under hydrogen at 973 K for 3 h, determined BET surface area 987 $m^2\,g^{-1}$; AC9, AC5 reduced with ammonia at 473 K, determined BET surface area 877 $m^2\,g^{-1}$. The BET surface area determination based on the N_2 adsorption isotherms is described elsewhere [22].

2.2. Photoreactor bench for standard degradation experiments

The experiments were carried out in a 1 l glass immersion photochemical reactor, charged with 800 ml of aqueous solution/suspension. The reactor was equipped with an UV lamp, located axially and held in a quartz immersion tube. The radiation source was a Heraeus TNN 15/32 low pressure mercury vapor lamp with an emission line at 253.7 nm (3 W of radiant flux). The solutions/suspensions were magnetically stirred. Typically irradiation was done in open air conditions with continuous stirring, which proved to supply enough oxygen for oxidative photodegradation. In case of need there was a feeding system connected to the reactor, for bubbling through the solution/suspension a controlled flow of an oxygen containing mixture at different partial pressures.

2.3. Photochemical degradation experiments

The SG dyestuff solutions were prepared by weighing the necessary amount of material and dissolving it to the desired volume of water. Solutions with an initial concentration ranging from 5 to 50 $mg\,l^{-1}$ were used throughout this study. Fresh solutions were prepared before use and diluted according to the requirements of the experiments. The reactor was feed with 800 ml of the solution, stirring was initiated and finally the source was turned on and the time count initiated. Samples (ca. 5 ml) were withdrawn at regular times for UV-Vis analysis.

2.4. Photocatalytical degradation experiments

During the experiments of UV irradiation in the presence of TiO_2 alone 1 $g\,l^{-1}$ suspensions of the semiconductor were used. The initial concentration of SG dyestuff was varied from 30 to 80 $mg\,l^{-1}$. Before illumination was turned on, the suspension was stirred for 30 min to let the solids adsorb the organic compound. A first sample was taken at the end of

the dark adsorption period, just before the light was turned on, in order to determine the concentration of dye in solution (non-adsorbed). Samples of the suspension were withdrawn regularly from the reactor and centrifuged immediately for separation of the suspended solids. The clean transparent solution was analyzed by UV-Vis spectroscopy as described in Section 2.5.

In the experiments involving the biphasic catalyst TiO_2 + AC, the AC prepared as described and ground just before use, was added to the TiO_2 suspensions. The concentrations used of AC and TiO_2 were 0.2 and 1 g l^{-1}, respectively, accounting for a 1/5 mass ratio. The initial concentration of SG dyestuff was varied from 20 to 60 mg l^{-1}. The prepared suspension was left to equilibrate for 30 min before light was turned on. The analysis of the samples followed exactly the same protocol as in the case of TiO_2 alone.

2.5. UV-Vis spectroscopic analysis

The UV-Vis spectrum of the SG dyestuff solutions and centrifuged samples was recorded on JASCO V-560 UV-Vis spectrophotometer, with a double monochromator, double beam optical system. The full spectra (250–750 nm) of the each sample was recorded and the absorbance at selected wavelengths registered. Repetition tests were made to ensure reproducibility. For kinetic analysis proposes each sample taken from the reactor was divided into three different vials and the final absorption was given by the arithmetic average over the three measurements.

The UV-Vis diffuse reflectance spectra of the solid (powder) materials was recorded on the same JASCO V-560 UV-Vis spectrophotometer equipped with an integrating sphere attachment (JASCO ISV-469). The powders were not diluted in any matrix to avoid a decrease of the absorbance. The reflectance spectra were converted by the instrument software (JASCO) to equivalent absorption Kubelka–Munk units.

2.6. DRIFT analysis

Diffuse reflection infrared Fourier transformed (DRIFT) spectroscopic analysis of the solid materials was done on a Nicolet 510P FTIR Spectrometer, with a KBr beam splitter for mid-IR range and a DTGS with KBr windows equipped with a special beam collector (COLLECTOR from Spectra Tech), fixed on a plate for consistent experimental conditions. The collection angle is a full pi steradians, collecting max 50% of the available diffuse energy and reducing the spot size of the FTIR beam by 1/6. When required the specular component was dealt with the blocker device, which minimizes the distortion. The instrument was always purged with dry air, which was passed through a filter to partially remove CO_2 and moisture (Balston air purifier with filter). Ground samples were used in a micro-cup and spectra taken at room temperature. Adequate background materials were chosen as appropriate. Typically there were recorded about 256 scans for each spectrum with a 4 cm^{-1} resolution. The interferograms were converted by the instrument software (OMINC) to equivalent absorption units in the Kubelka–Munk scale.

3. Results and discussion

3.1. Photolytic degradation by UV radiation

The degradation curves of the SG dyestuff by UV radiation are well fitted by a mono-exponential curve, suggesting that a pseudo-first-order homogeneous reaction model can be taken in consideration for describing the kinetic behavior. Considering that the UV radiation is the sole responsible for dyestuff bleaching from the solution, according to Eqs. (1) and (2) and considering that the limiting step is the scission of the starting material the kinetic equation that describes the process is

$$-\frac{dC}{dt} = k_{UV}C \tag{7}$$

with k_{UV} the pseudo-first-order rate constant and C the concentration of SG BLE 155 in each moment where $t > 0$.

Integration of Eq. (7), with the usual restriction of $C = C_0$ at $t = 0$, will lead to a linear plot of $\ln(C_0/C)$ versus t with a slope of k_{UV} the pseudo-first-order rate constant (Fig. 2).

The photodegradation experiments under conditions of constant UV irradiating flux for different initial concentrations of dyestuff, show a variation in the k_{UV} values (Table 1). A 10-fold increase in the initial concentration of the SG dyestuff leads to a 6-fold decrease on the rate constant of the process. The observed decrease on k_{UV} as the initial concentration of the dyestuff increases can be explained in terms of the less availability of photons as the color of the solution gets more intense.

At the reaction conditions, it is reasonable to assume that photon absorption is instantaneous compared to bond scission, since the lifetime of the excited state is normally stabilized by solvent interaction. In the presence of an external oxidizing agent in large excess, such as molecular oxygen, this excited state will be quenched at diffusion rate according to Eq. (1). This will result in a similar rate law, replacing in Eq. (7) k_{UV} by $k_{app} = k[O_2]$, taking in account Eqs. (1)–(3), considering k the second-order rate constant for the diffusion

Table 1
Apparent first-order kinetic rate constants (k_{UV}) and conversion at 15 min after turning on illumination (χ_{15}) in net photochemical experiments with different initial concentrations of SG dyestuff

C_0 (mg l^{-1})	k_{UV} (min^{-1})	χ_{15} (%)
50	0.042	48
30	0.068	66
20	0.086	75
10	0.18	92
5	0.27	93

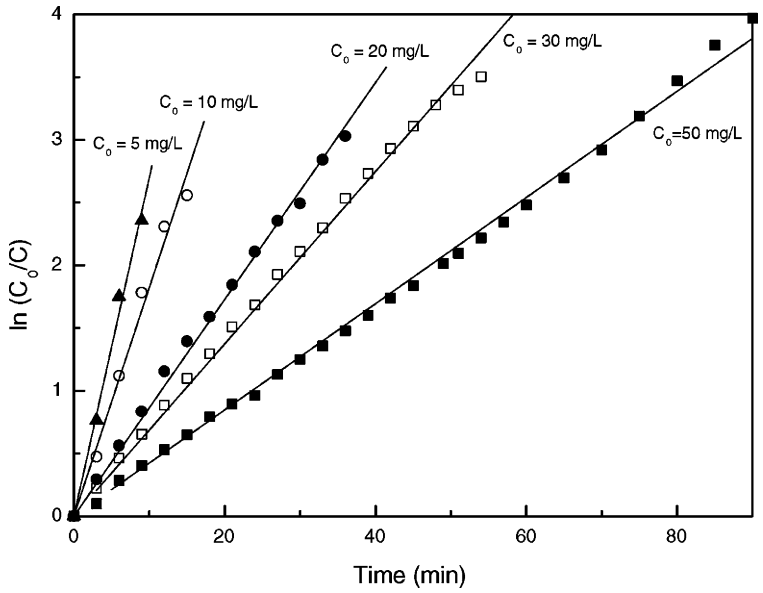

Fig. 2. Kinetics of SG dyestuff degradation (linear transform $\ln C_0/C$ vs. t) in net photochemical experiments for different initial concentrations ((▲) $C_0 = 5\,\mathrm{mg\,l^{-1}}$; (○) $C_0 = 10\ \mathrm{mg\,l^{-1}}$; (●) $C_0 = 20\ \mathrm{mg\,l^{-1}}$; (□) $C_0 = 30\ \mathrm{mg\,l^{-1}}$; (■) $C_0 = 50\ \mathrm{mg\,l^{-1}}$).

process (Eq. (3)) and assuming that the oxygen concentration is kept constant during the process. Experiments made where the oxygen partial pressure was increased five times, show no effect on the apparent rate constant (k_{app}), which leads to the conclusion that the reaction rate of degradation is of pseudo-zero-order in oxygen.

3.2. Photocatalytic degradation in water by TiO_2

The results from Section 3.1 clearly show that direct photolysis cannot be excluded when studying the degradation process by the UV radiation. As showed, in the absence of TiO_2 (neat *photochemical* regime) there is a significant degradation of the dyestuff. In this case, it is clear that the system containing TiO_2 could not be working in a pure *photocatalytical* regime. Nevertheless, since the photochemical regime is characterized, it is possible to obtain meaningful information about the photocatalyitc process.

The degradation experiments by UV irradiation of SG BLE 155 aqueous solutions containing TiO_2 follow identical pseudo-first-order kinetics with respect to the concentration of the dyestuff in the bulk solution (C):

$$-\frac{dC}{dt} = k_{app}C \tag{8}$$

Integration of that equation (with the same restriction of $C = C_0$ at $t = 0$, with C_0 being the initial concentration in the bulk solution after dark adsorption) will lead to the expected relation:

$$\ln\left(\frac{C_0}{C}\right) = k_{app}t \tag{9}$$

in which k_{app} is the apparent first-order rate constant and t the reaction time. A plot of $\ln(C_0/C)$ versus t for all the experiments with different initial bulk concentration of dyestuff is shown in Fig. 3. The values of k_{app} can be obtained directly from the regression analysis of the curves in the plot (Table 2).

The initial concentration of the dyestuff (C_0') was observed to decrease after a period of dark adsorption. Preliminary kinetic analysis showed that the equilibrium was reached after 15 min time. Therefore, for kinetic analysis of the photochemical experiments the initial concentration (C_0) was taken as the concentration of the dyestuff in solution, determined by the absorption of the aqueous solution (centrifuged) after 30 min time (Table 2). This initial concentration of the dyestuff has a fundamental effect on the degradation rate, i.e. the kinetic rate constant decreases with the concentration. Or from a practical standpoint, at the same illumination time the relative amount of SG dyestuff decomposed is less for the more heavy colored solutions.

The adsorption of SG dyestuff on TiO_2 was characterized by means of the variation in the infrared spectrum of the semiconductor (Fig. 4). Comparing the spectrum of the pure TiO_2 (Fig. 4A) with that of the same material after the 30 min

Table 2
Apparent first-order kinetic rate constants (k_{app}) and conversion at 15 min after turning on illumination (χ_{15}) in photocatalytic experiments using TiO_2 with different initial concentrations of SG dyestuff before (C_0') and after (C_0) dark adsorption

C_0' ($\mathrm{mg\,l^{-1}}$)	C_0 ($\mathrm{mg\,l^{-1}}$)	k_{app} ($\mathrm{min^{-1}}$)	χ_{15} (%)
80	49	0.024	27
60	34	0.039	41
50	20	0.047	48
40	11	0.072	71
30	8	0.078	72

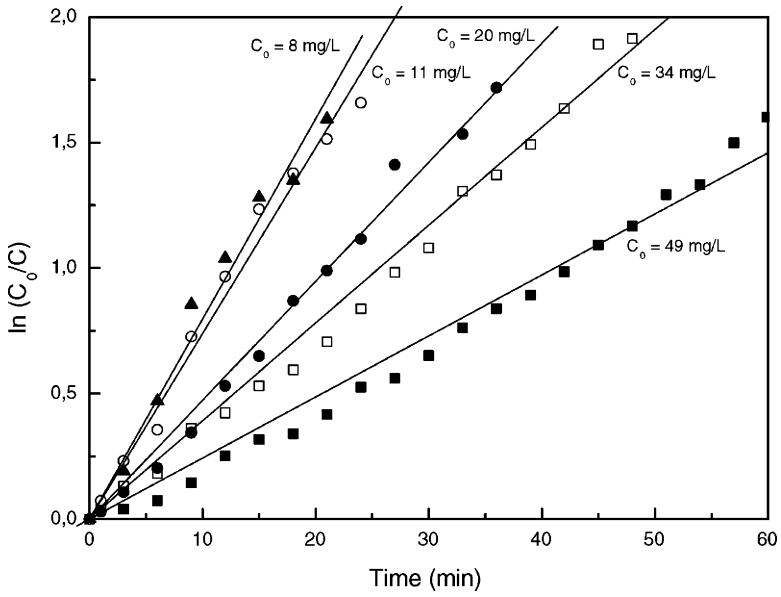

Fig. 3. Kinetics of SG dyestuff degradation (linear transform $\ln(C_0/C)$ vs. t) in photocatalytic experiments using TiO_2 for different initial concentrations of the dyestuff ((▲) $C_0 = 8$ mg l^{-1}; (○) $C_0 = 11$ mg l^{-1}; (●) $C_0 = 20$ mg l^{-1}; (□) $C_0 = 34$ mg l^{-1}; (■) $C_0 = 49$ mg l^{-1}).

time of black adsorption (Fig. 4B), it is visible the difference due to the adsorption of the dyestuff. The new bands visible in the region 1660–1000 cm^{-1} can be ascribed to the different functional groups of the dye. The 1300–1000 cm^{-1} region includes the vibrational modes of the aromatic structure of the dye that are obscured by some bands from the azo and amino substituents. The characteristic N=N stretching mode [23] in the vibrational spectrum gives rise to the peaks in the region 1504–1478 and 1413 cm^{-1}, with some loss of definition due to existence of three different types of azo bonds in the compound. The resolution of the spectra is

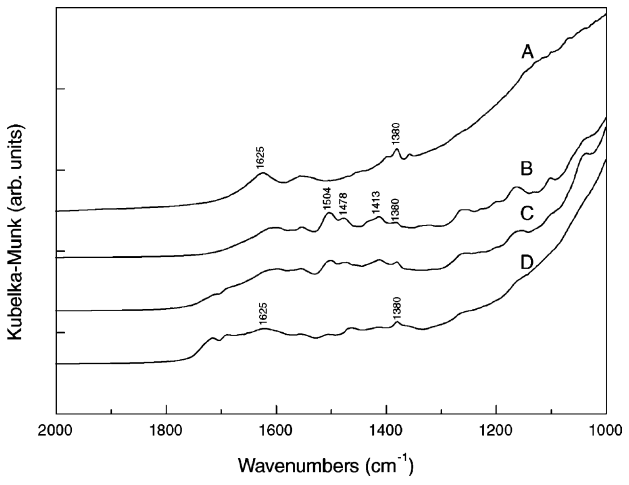

Fig. 4. Diffuse reflectance infrared Fourier transformed (DRIFT) spectra of the catalyst TiO_2 during several steps in the photocatalytic experiment with a $C_0' = 50$ mg l^{-1} of SG dyestuff. (A) TiO_2 naked catalyst; (B) TiO_2 sample at the end of the 30 min dark adsorption period; (C) TiO_2 sample at 30 min after turning on illumination; (D) TiO_2 sample at the end of the reaction, 120 min.

partially lost after 30 min of reaction time as the azo bands change in intensity (Fig. 4C). Visually, it was confirmed that as the reaction time increases the color of the aqueous solution faints. The 1504–1478 and 1413 cm^{-1} bands and are completely removed at the end of the reaction (Fig. 4D), but the resolution of the spectrum is not recovered. This can be attributed to fact that the N=N bonds are being efficiently broken and consequently the dye degraded. Parallel to this degradation, there is also a change in the vibrational structure of the TiO_2, as the bands at 1625 and 1380 cm^{-1} are getting less defined. Finally, when the color is completely removed from the solution the bands characteristic of the SG dyestuff disappeared, although some color was retained by the TiO_2. This is confirmed by comparing the spectra of the initial TiO_2 (Fig. 4A) to that after the reaction (Fig. 4D) there is no perfect match between them which can derived from eventual adsorption of degradation products.

Under the experimental conditions, taking in account the amount of dyestuff present in solution after dark adsorption, it can be calculated that >95% of the incident photons are absorbed by the TiO_2. Which means that we are basically in the presence of a heterogeneous photocatalyitc process and the experimental results can be explained in terms of two elementary mechanisms: (i) oxidation of the dyestuff through successive attacks by the hydroxyl radical ($HO^{\bullet}$); (ii) direct reaction of the dyestuff with photogenerated holes in a process similar to the photo-Kolbe reaction [24]. The first process requires that the dyestuff molecules and the other oxygen containing species adsorb in neighbor sites. Oxygen is in fact omnipresent on the TiO_2 surface and in its molecular form acts as electron acceptor, contributing via the superoxide radical ($O_2^{\bullet -}$) to the formation of hydrodioxyl radical ($HO_2^{\bullet}$) which is a known intermediate for

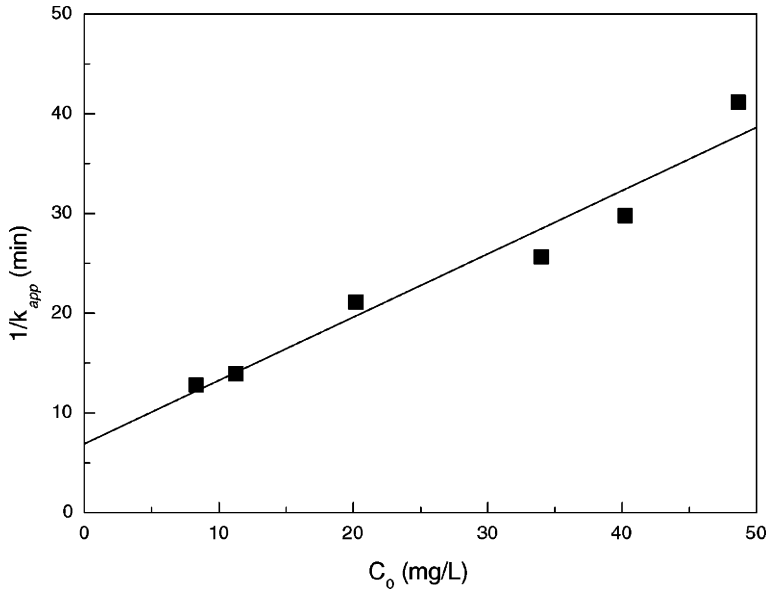

Fig. 5. Determination of the adsorption equilibrium constant, K_C, and the reaction rate constant, k_C following the modified Langmuir–Hinshelwood kinetic model.

the HO• radical [13]. However, the HO• radical should be mainly formed from the adsorbed OH^- and H_2O molecules by electron donation to the photogenerated holes. Considering the above processes, the reaction rate for surface decomposition of SG dyestuff may be written as the sum of the contributions of a Langmuir–Hinshelwood type of kinetics and a first-order decomposition following direct bond breaking at the TiO_2 surface:

$$r = k''\vartheta_{HO}\vartheta_{SG} + k'\vartheta_{SG} \quad (10)$$

where k' and k'' are, respectively, the first and second-order surface rate constants, ϑ_{HO} the fractional site coverage by HO• radicals and ϑ_{SG} the fraction of sites covered by SG dyestuff. Owing to the fact that water is the solvent (i.e. H_2O and OH^- are in large excess) and the oxygen partial pressure remains the same in a given experiment, the fractional site coverage by HO• radicals is also constant, and Eq. (10) can be arranged as

$$r = k_{HO}\vartheta_{SG} + k'\vartheta_{SG} \quad (11)$$

with k_{HO} includes the second-order rate constant. On the other hand, the fractional site coverage by the SG dyestuff is given by

$$\vartheta_{SG} = \frac{K_C C}{1 + K_C C + \sum_i K_i[I_i]} \quad (12)$$

in which K_C and K_i are equilibrium adsorption constants and "I" refers to the various intermediate products of SG degradation. If it assumed that the adsorption coefficients for all organic molecules present in the reacting mixture are effectively equal, the following assumption can be made:

$$K_C C + \sum_i K_i[I_i] = K_C C_0 \quad (13)$$

where C_0 is the initial concentration of SG BLE 155. Now substitution of Eq. (12) into Eq. (11) results on the expression

$$r = k_C \frac{K_C C}{1 + K_C C_0} = k_{app} C \quad (14)$$

with $k_C = k_{HO} + k'$. The relationship between k_{app} and C_0 can be expressed as a linear equation:

$$\frac{1}{k_{app}} = \frac{1}{k_C K_C} + \frac{C_0}{k_C} \quad (15)$$

In Fig. 5 is shown a plot of $1/k_{app}$ versus C_0. The values of the adsorption equilibrium constant, K_C, and the rate constant, k_C, were obtained by linear regression of the points calculated by Eq. (15). The values were $K_C = 0.0923\,l\,mg^{-1}$ and $k_C = 1.58\,mg\,l^{-1}\,min^{-1}$.

3.3. Photocatalytic degradation in water by TiO_2 and activated carbon

The kinetics of color removal of the dyestuff solution containing the mixtures of TiO_2 and the activated carbons followed an apparent first-order rate, so it is reasonable to evaluate the efficiency of degradation based on the apparent first-order rate constant of the process. The extent of the effect was quantified in terms of a synergy factor, R ($R = k_{app}(TiO_2 + AC)/k_{app}(TiO_2)$) as suggested in the previous literature [20]. For solutions with the typical concentration of dyestuff around $50\,mg\,l^{-1}$, and a mass ratio AC/TiO_2 of 1/5, a systematic increase on the first-order constant was observed, although with different magnitudes (Table 3). The ROX 0.8 activated carbon (AC3) used before with success as support for noble metal catalysts in the catalytic wet air

Table 3
Apparent first-order kinetic rate constants (k_{app}) and synergy factor (R) in photocatalytic experiments using mixtures of TiO_2 and different activated carbons (AC) for different initial concentrations of SG dyestuff before (C_0') and after (C_0) dark adsorption

Catalyst	C_0' (mg l^{-1})	C_0 (mg l^{-1})	k_{app} (min^{-1})	R
TiO_2	80	49	0.0243	–
TiO_2 + AC1	60	44	0.0475	2.0
TiO_2 + AC2	70	44	0.0382	1.6
TiO_2 + AC3	70	46	0.0457	1.9
TiO_2 + AC4	70	42	0.0435	1.8
TiO_2 + AC5	75	41	0.0245	1.0
TiO_2 + AC6	80	42	0.0276	1.1
TiO_2 + AC7	75	50	0.0371	1.5
TiO_2 + AC8	75	50	0.0389	1.6
TiO_2 + AC9	73	43	0.0403	1.7

oxidation of model compound pollutants [25], was tested after different type of liquid phase treatments, which consisted mainly in chemical high temperature activation. The liquid phase activation treatments here employed are know to increase the acidity of the activated carbon surface due to a substantial increase in the carboxylic acid and anhydride type of functional groups (other groups such as phenol, and lactone are also present in significant amounts). This type of treatment is know to have no significant impact on the textural properties of this type carbon materials [26], although some decrease in the BET surface area is actually observed. The results (Table 3) show that no significant increase in R is visible on the treated ROX 0.8 carbons relative to the non-treated commercial AC3, meaning that the development of an acidic surface on the carbon rich in carboxylic acid groups does not increase the photoefficiency of the process. In fact, it is observed that the best results are obtained for the samples oxidized with H_2O_2 (AC4) which normally provides a milder oxidation and lesser acidic carbon surface. It is noticeable that the sample oxidized with nitric acid 5 M, without any further treatment (AC5) shows no synergy factor at all. It should be stressed that the R factor is not proportional to the textural properties of the modified carbons. Looking at the set of modified carbons composed by AC5, AC6 and AC9, the first ones were high temperature modified, have the smaller surface area, and display an R factor of 1.0–1.1; the last was modified at low temperature, resulting in an intermediate surface area and displays an R factor of 1.7.

The GAC 1240 PLUS (AC2) is an acid washed granular activated carbon produced by steam activation and shows a R factor of 1.6.

Comparing all the different brands of AC, the more positive effect ($R = 2.0$) was observed for the C-GRAN carbon (AC1). This carbon has a very open (macro/mesopore) structure, being specially effective adsorbing higher molecule weight organics. It has a special surface chemistry resulting from a controlled chemical activation, using the phosphoric acid process. From the present results, it follows the conclusion that the surface properties of the AC are determinant for the observed photoefficiency.

For the materials used (TiO_2, AC1 and TiO_2 + AC1) the diffuse reflectance spectra expressed in terms of Kubelka–Munk equivalent absorption units are presented in Fig. 6. As expected TiO_2 has no absorption above its fundamental absorption sharp edge raising at 400 nm. On the other hand, for the AC1 the absorption is total over the all range of the UV-Vis spectrum. The TiO_2 + AC1 catalytic system shows basically the same absorption pattern as the bare TiO_2. At wavelengths below 320 nm the two spectra are identical. For the rest of the spectrum there is an increase

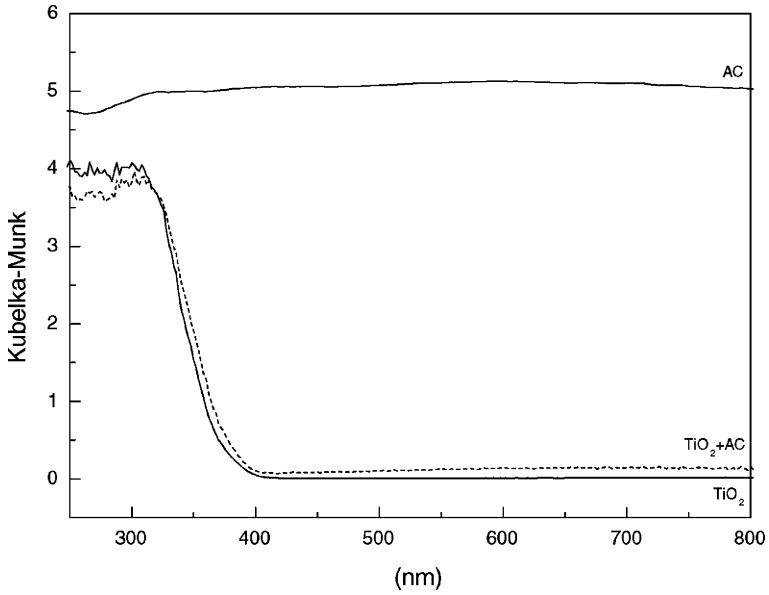

Fig. 6. Diffuse reflectance electronic absorption spectra of the activated carbon AC1, the naked catalyst TiO_2 and the mixed catalyst TiO_2 + AC1.

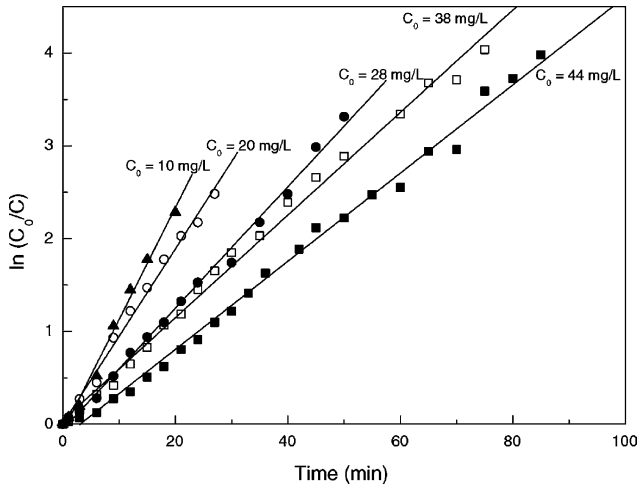

Fig. 7. Kinetics of SG dyestuff degradation (linear transform $\ln(C_0/C)$ vs. t) in photocatalytic experiments using TiO_2 + AC1 for different initial concentrations of the dyestuff ((▲) $C_0 = 10\,mg\,l^{-1}$; (○) $C_0 = 20\ mg\,l^{-1}$; (●) $C_0 = 28\ mg\,l^{-1}$; (□) $C_0 = 38\ mg\,l^{-1}$; (■) $C_0 = 44\ mg\,l^{-1}$).

in the residual absorption on the visible range, together with a slight onset of the diffuse reflectance spectrum to the red. These observations lead to the conclusion that the fundamental process of electron/hole pair formation should apply, the energetics of the process being slightly changed due to the experiential onset. Since, the irradiation is carried on with the 253.7 nm light, the change in the visible part of the spectrum should not interfere with the photocatalytic process.

Following the absorption of the aqueous solution ($\lambda = 610$ nm), after centrifugation of the suspension containing TiO_2 + AC1, the calculated plot of $\ln(C_0/C)$ versus t gives straight lines for all the experiments with different initial concentration of dyestuff as shown in Fig. 7. From the slopes, apparent first-order rate constant values of k_{app} can be obtained (Table 4). Considering the description of the kinetic behavior in terms of a modified Lagmuir–Hinshelwood model as discussed in Section 3.2 (in agreement with a surface reaction), a first-order kinetic equation with respect to dye concentration will be obtained, exactly the same as in Eq. (14). A plot of the $1/k_{obs}$ versus C_0 will follow a linear relationship (as in Eq. (15)) and the values of the adsorption equilibrium constant, K_C, and the rate constant, k_C, obtained by linear regression of the experimental are $0.0928\,l\,mg^{-1}$ and $2.64\,mg\,l^{-1}\,min^{-1}$, respectively.

Table 4
Apparent first-order kinetic rate constants (k_{app}) and conversion at 15 min after turning on illumination (χ_{15}) in photocatalytic experiments using TiO_2 + AC1 with different initial concentrations of SG dyestuff before (C_0') and after (C_0) dark adsorption

C_0' ($mg\,l^{-1}$)	C_0 ($mg\,l^{-1}$)	k_{app} (min^{-1})	χ_{15} (%)
60	44	0.048	40
50	38	0.055	56
40	28	0.065	61
30	20	0.094	77
20	10	0.120	83

It is to be noticed that while the kinetic rate constant increased (relative to the TiO_2 alone situation), the values of K_C are comparable in the cases of TiO_2 and TiO_2 + AC1 suggesting that the thermodynamics of adsorption are similar, the difference being in the kinetics of the process. The conclusion that follows is that the AC does not dramatically change the adsorption properties of the resulting catalyst with relation to the initial pollutant molecule, but it plays an important role in the kinetics of the photocatalytic process.

The concentration of dyestuff on the aqueous solutions containing TiO_2 + AC1 (Table 4), after the 30 min period of dark adsorption, is comparable to that of TiO_2 alone (Table 2), which means that no additive effect is obtained in the absorption capacities of both materials. In fact the observation that the amount of SG dyestuff adsorbed in the TiO_2+ AC1 suspensions is even lower to that observed in the TiO_2 case, suggests a reduction of the number of active sites of adsorption in the presence of such effective adsorbent which is the C-GRAN. It is remarkable that the inclusion of an activated carbon material, a very efficient co-adsorbent, does not increase the adsorption ability of the semiconductor support. This sustains of the explanation advanced previously based on the creation of an interface between TiO_2 and AC at which SG BLE 155 molecules cannot adsorb [10]. However, it must be stressed that as the initial SG dyestuff concentration increases the fractional coverage also increases for the same AC/TiO_2 ratio; for the $30\,mg\,l^{-1}$ concentration the amount of non-adsorbed material increases by a factor 2.5 while the common interface can be estimated to account for a reduction of 3–30% of the total area of catalyst [10]. Mass transfer limitations are not likely to interfere because during the entire experiment the solution is stirred. It was confirmed that different stirring speeds had no effect on the kinetics.

On the other hand, it was verified (not a detailed kinetic experiment) that the kinetic rate constant increases with the partial pressure of oxygen, showing that oxygen plays a major role in the photodegradation of SG dyestuff.

From the results here presented it can be concluded that the chemical nature of the AC and the presence of oxygen are determinant for the degradation process, which can be explained in terms of two different mechanisms:

1. The SG dyestuff adsorption on the AC is followed by a transfer of the compound to the TiO_2 where undergoes a photocatalyzed surface reaction of degradation. The driving force for this transfer is probably the difference in the dye concentration between AC and TiO_2 causing surface diffusion of the dye to TiO_2.
2. The AC acts as a photosensitizer which injects an electron in the conduction band of TiO_2 and triggers the photocatalytic formation of the very reactive $HO^{\bullet}$ radical, which is responsible for the degradation of the dye.

While the first mechanism has been discussed in relation with systems similar to the ones here described [10,20,21],

the second was proposed for coke-containing TiO_2 catalysts [27], conceptually very different from the present ones. In the case of the first mechanism degradation may proceed via the process described in Eq. (6), or also trough reaction with the $HO^{\bullet}$ radical formed by the process described n Eqs. (4) and (5). The later will justify the necessity of oxygen in the overall degradation process.

The AC tested here are typically used for adsorption of large organic molecules, including several type of dyes. Preliminary investigations on an extensive set of dyes, including the one used in the present study, do show that the kinetics of the adsorption over AC are in fact slower than over TiO_2. Based on this result, 30 min was the time length chosen for the period of dark adsorption. In this way it was ensured that the adsorption over the AC will not compete significantly with TiO_2. Additionally, it was noted that AC with identical textural properties favoring the adsorption of large dye molecules, display different behaviors towards the same dye depending on chemistry of the surface. In view of all these results, the contribution of the first of the two proposed mechanisms described in the previous paragraphs, is expected to be less important. The AC systems with best performances are the ones were the surface is basic, or slightly acid (from a Lewis standpoint), therefore the ones with some electron availability. This is in line with the possibility of an electron transfer process from the carbon to the TiO_2 conduction band, as suggested by the second mechanism. The electronic changes observed in the diffuse reflectance spectrum of the TiO_2 + AC1, are also in agreement with a decrease of the band gap of the semiconductor favoring the process of electron transfer to the conduction band.

3.4. Comparison of the photoinduced processes for degradation of the SG dyestuff

A global comparison between the kinetic rate constants for three oxidation systems is show in Fig. 8. From the analysis of the results presented there is clear that for the for aqueous solutions with a low dye content (not heavily colored) the photolytic degradation is by far the most efficient process. This is not surprising in view of the particular nature of the azo dyes: the N=N bond is conjugated with the aromatic system and upon excitation of the molecule becomes very labile. As the dye concentration increases the heavy coloration and formation of agglomerates play a role inhibiting the photolytic process. As the concentration of the dye increases approaching values typically found in textile washing baths, the efficiency of the processes levels down, with an advantage to the TiO_2 + AC system. Globally, the results show that there is a relationship between the initial concentration of the dye in the solution and the rate of its degradation: as the concentration of the initial solution raises the dye degradation process becomes slower, which is attributable to the inner filter effect for the photochemical process, and to the decrease of the relationship active sites per organic molecule in the case of the photocatalytic experiments. Actually a synergy effect

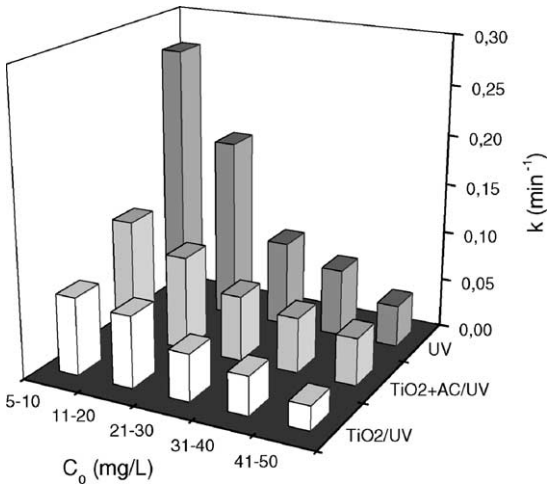

Fig. 8. Comparison of the apparent first-order rate constants for the kinetics of color removal on the dyestuff solutions with different initial concentrations, without TiO_2, with TiO_2 alone and with mixtures of TiO_2 + AC1.

due to the introduction of the AC is visible over the all range of dye concentration for the photocatalytic process (Fig. 8).

4. Conclusions

Photochemical degradation of an azo dye can be achieved efficiently by three different processes. Direct UV irradiation is very effective at low dye concentrations, but for heavily colored systems a photocatalytic process is more efficient. Irrespective of the process chosen a color removal of practically 100% was always possible. The experimental results indicated that the kinetics of three degradation processes, UV, TiO_2/UV and TiO_2 + AC/UV, fit well a pseudo-first-order kinetic disappearance, which means that from a practical standpoint it is possible to obtain decolored water in a convenient time scale. The photocatalytic degradation processes can be explained in terms of a modified Langmuir–Hinshelwood model for the surface reaction between the dyestuff and the oxidizing agent. The values of the adsorption equilibrium constants, K_C, and the second-order rate constants, k_C, were $0.0923\,l\,mg^{-1}$ and $1.58\,mg\,l^{-1}\,min^{-1}$ for the TiO_2/UV process and $0.0928\,l\,mg^{-1}$ and $2.64\,mg\,l^{-1}\,min^{-1}$ for TiO_2 + AC/UV system, respectively. The addition of powdered activated carbon to TiO_2 under UV irradiation induces a beneficial effect on the photocatalytic degradation of SG BLE 155. Both, the presence of oxygen and the chemical nature of the AC surface are found to be important in the photoefficiency of the process.

From an applied standpoint, this result shows that even for a model solution containing no other than the dyestuff, the efficiency of water cleaning is strongly dependent on its concentration in the stream. In the case of very heavy colored streams the fact of having a adsorbing material, with

catalytic properties, will be advantageous when UV radiation is to be considered. UV radiation sources are able to delivery energy very efficiently using low lamp power and match the band gap requirements of a simple active carbon modified TiO_2.

Acknowledgements

The authors wish to thank Dr. M.F. Pereira (LCM/DEQ–FEUP), for supplying some of the activated carbons and for some useful comments. To Dr. R.A. Boaventura (LSRE-FEUP) for the samples of dyestuff. To NORIT Nederland B.V. for the commercial activated carbon. This research was carried out under the plan of actions of project POCTI/33401/EQU/2000, approved by the Fundação para a Ciência e a Tecnologia (FCT), Programa Operacional (POCTI), and co-supported by FEDER.

References

[1] O. Legrini, E. Oliveros, M. Braun, Chem. Rev. 93 (1993) 671.
[2] R. Andreozzi, V. Caprio, A. Insola, R. Marotta, Catal. Today 53 (1999) 51.
[3] J.-M. Herrmann, Catal. Today 53 (1999) 115.
[4] S.N. Frank, A.J. Bard, J. Am. Chem. Soc. 99 (1977) 303.
[5] S.N. Frank, A.J. Bard, J. Phys. Chem. 81 (1977) 1484.
[6] A. Mills, S. Le Hunte, J. Photochem. Photobiol. A: Chem. 108 (1997) 1.
[7] A. Fujishima, T.N. Rao, D.A. Tryk, J. Photochem. Photobiol. C 1 (2000) 1.
[8] N. Serpone, A. Salinaro, Pure Appl. Chem. 71 (1999) 303.
[9] A. Salinaro, A.V. Emeline, J. Zhao, H. Hidaka, V.K. Ryabchuk, N. Serpone, Pure Appl. Chem. 71 (1999) 321.
[10] J. Matos, J. Laine, J.-M. Herrmann, J. Catal. 200 (2001) 10.
[11] K. Hunger, P. Mischke, W. Rieper, R. Raue, K. Kunde, A. Engel, in: Ullmann's Encyclopedia of Industrial Chemistry—Electronic Release, Wiley, Germany, 2002.
[12] H. Zollinger (Ed.), Color Chemistry: Synthesis, Properties and Applications of Organic Dyes and Pigments, VCH, NY, 1991.
[13] M. Vautier, C. Guillard, J.-M. Herrmann, J. Catal. 201 (2001) 46.
[14] A. Houas, H. Lachheb, M. Ksibi, E. Elaloui, C. Guillard, J.-M. Herrmann, Appl. Catal. B 31 (2001) 145.
[15] C. Galindo, P. Jacques, A. Kalt, J. Photochem. Photobiol. A: Chem. 141 (2001) 47.
[16] C. Bauer, P. Jacques, A. Kalt, J. Photochem. Photobiol. A: Chem. 140 (2001) 87.
[17] N. Takeda, T. Torimoto, S. Sampath, S. Kuwabata, H. Yoneyama, J. Phys. Chem. 99 (1995) 9986.
[18] T. Torimoto, S. Ito, S. Kuwabata, H. Yoneyama, Environ. Sci. Technol. 30 (1996) 1275.
[19] T. Torimoto, Y. Okawa, N. Takeda, H. Yoneyama, J. Photochem. Photobiol. A: Chem. 103 (1997) 153.
[20] J. Matos, J. Laine, J.M. Herrmann, Appl. Catal. B 18 (1998) 281.
[21] J. Matos, J. Laine, J.M. Herrmann, Carbon 37 (1999) 1870.
[22] M.F.R. Pereira, S.F. Soares, J.J.M. Orfão, J.L. Figueiredo, Carbon, in press.
[23] D. Lin-Vien, N.B. Colthup, W.G. Fateley, J.G. Grasselli, in: The Handbook of Infrared and Raman Characteristic Frequencies of Organic Molecules, Academic Press, Boston, 1991.
[24] B. Krauetler, A.J. Bard, J. Am. Chem. Soc. 99 (1977) 7729.
[25] H.T. Gomes, J.L. Figueiredo, J.L. Faria, Appl. Catal. B 27 (2000) L217.
[26] J.L. Figueiredo, M.F.R. Pereira, M.M.A. Freitas, J.J.M. Orfao, Carbon 37 (1999) 1379.
[27] C. Lettmann, K. Hildenbrand, H. Kisch, W. Macyk, W.F. Maier, Appl. Catal. B 32 (2001) 215.